

Magnetization and the phase diagram of CuGeO_3 doped with 2% Zn

This article has been downloaded from IOPscience. Please scroll down to see the full text article.

1998 J. Phys.: Condens. Matter 10 10215

(<http://iopscience.iop.org/0953-8984/10/45/009>)

View [the table of contents for this issue](#), or go to the [journal homepage](#) for more

Download details:

IP Address: 171.66.16.210

The article was downloaded on 14/05/2010 at 17:49

Please note that [terms and conditions apply](#).

Magnetization and the phase diagram of CuGeO_3 doped with 2% Zn

M Saint-Paul[†], J Voiron[‡], C Paulsen[†], P Monceau[†], G Dhalenne[§] and A Revcolevschi[§]

[†] Centre de Recherches sur les Très Basses Températures, Laboratoire associé à l'Université Joseph Fourier, CNRS, BP 166, 38042 Grenoble Cédex 9, France

[‡] Laboratoire Louis Néel, CNRS, BP 166, 38042 Grenoble Cédex 9, France

[§] Laboratoire de Chimie des Solides, Université Paris-Sud, 91405 Orsay, France

Received 27 July 1998

Abstract. We report on magnetization measurements as a function of temperature between 0.1 and 10 K for $\text{Cu}_{0.98}\text{Zn}_{0.02}\text{GeO}_3$ single crystals in a magnetic field up to 14 T. The successive antiferromagnetic order and the spin–Peierls (SP) transition are confirmed. In the SP state, the paramagnetic contribution due to the spins induced by impurities corresponds to one spin 1/2 per Zn atom. The very specific nature of the low-temperature antiferromagnetic state coexisting with the dimerized spin–Peierls state is also revealed in the magnetization curves.

1. Introduction

In the last few years, the quasi-one-dimensional (Q-1D) Cu^{2+} ($S = \frac{1}{2}$) antiferromagnet CuGeO_3 has been intensively studied [1]. This compound undergoes a spin–Peierls (SP) transition which is driven by the interaction between 1D antiferromagnetic chains and the 3D phonon field. As a result of substitution at the cationic site, the lattice and exchange interactions between Cu^{2+} spins are modified, resulting in a competition between the lattice dimerization and the 3D antiferromagnetic (AF) ordering [2]. The coexistence at low temperatures of the SF and AF states has been demonstrated by neutron scattering experiments on Zn-doped [3–5, 7] and Si-doped [3, 6, 7] crystals. Such a coexistence between two order parameters, supposed exclusive, is possible due to the very specific nature of the SP ground state. This latter results from the coupling between the 1D antiferromagnetic order and the crystal lattice which induces a dimerization of the magnetic ions leading to the formation of a non-magnetic singlet ground state [1]. But the quantum coherence of this singlet ground state is very sensitive to any disorder, which can affect it and consequently reveal the magnetic properties of the spins from which it is formed. Using a phase Hamiltonian, it was shown that lattice distortion and staggered moments may have a long-range order but with spatial modulations: the lattice dimerization is reduced at the impurity site and the staggered magnetic moments extend to a soliton size of a few lattice constants [8]. A similar model was also proposed in which the localized spins released by impurities are antiferromagnetically coupled by the polarization of the singlet background [9]. These models indicate that the dimerization sustains the coherence of the AF phase of the spin polarization and that there is no critical impurity concentration for the occurrence of the AF state. Thus it was recently shown that AF order appears in $\text{Cu}_{1-x}\text{Zn}_x\text{GeO}_3$ below

28 mK for $x \sim 5 \times 10^{-3}$ [10]. On the other hand, if the number of impurities is increased, the SP transition temperature decreases and the coupling between the AF moments may lead to a conventional AF Néel state, without SP lattice distortion, as shown from specific heat measurements for Si-doped CuGeO_3 with $x = 0.02$ ($T_N \sim 4.5$ K) [11].

The magnetic phase diagram of doped CuGeO_3 has general features which do not crucially depend on the type of dopant; it has been derived from neutron scattering [3–7], magnetization [2, 12–14], specific heat [11] and ultrasound measurements [15–17]. The phase diagram includes the uniform (U) phase, the dimerized (D) phase, the AF phase at low temperature and the magnetic incommensurate (I) phase which appears above a critical magnetic field. The existence of the I phase above 10 T was proved by x-ray measurements performed on Zn-doped [18] and Si-doped [7] crystals. From our ultrasound measurements on a 2% Zn-doped crystal [17], we have shown that the I phase is situated in an area of the phase diagram demarcated by three lines as shown in figure 1: the I–U, I–D and I–I' lines. The I–I' and I–U lines merge together at $H = 15$ T and $T = 5$ K. Above 15 T up to 20 T, the transition line between phases U and I' is nearly temperature independent. The I'–I line has also been detected up to 14 T by ultrasound measurements on a 1–5% Zn-doped crystal [16] and by specific heat measurements up to 15 T on a 1% Si-doped crystal [11]. It also appears that the transition lines between the AF and SP states and between the commensurate and incommensurate phases cross at a ‘tetracritical’ point located at 9 T and 2 K for the 2% Zn-doped crystal (figure 1).

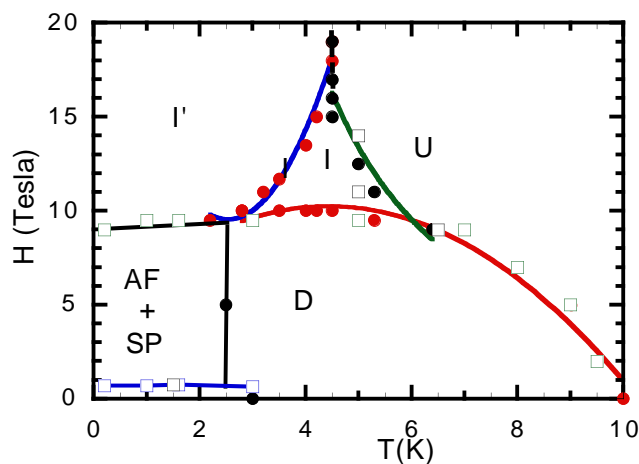


Figure 1. The magnetic phase diagram of $\text{Cu}_{0.98}\text{Zn}_{0.02}\text{GeO}_3$. The open squares represent the critical fields determined from the magnetization measurements. The solid lines were obtained from sound velocity measurements [17].

The nature of the I' phase and its difference from the I phase are not well understood. Thus our aim was, by measuring the magnetization of a 2% Zn-doped crystal, first to follow the I–D transition line at low temperature in the AF phase and, second, to detect any change occurring at the I'–I transition line.

2. Experimental procedure and results

The $\text{Cu}_{0.98}\text{Zn}_{0.02}\text{GeO}_3$ single crystal used in this study was cut from a large crystal several centimetres long grown from the melt by a floating-zone method associated with an image

furnace [19]. The magnetization was measured by the standard extraction method in magnetic fields up to 14 T applied parallel to the c -axis. The same sample as for the ultrasound measurements [17] was used. A dilution refrigerator was also used for the measurements below 1.5 K.

2.1. The AF-I' transition line

Curves showing the field dependence of the magnetization, M , measured at 90 mK, 200 mK, 1 K and 1.6 K are drawn in figure 2. Two magnetization jumps are observed; the AF-I' phase transition line is associated with the large change of the slope dM/dH at the critical field $H_c \sim 9.5$ T.

A spin-flop transition occurs at 0.7 T as shown in the inset of figure 2 for temperatures of 0.2 and 0.9 K. A similar spin-flop transition had already been reported for Si-doped CuGeO_3 [15] at the same field of about 1 T.

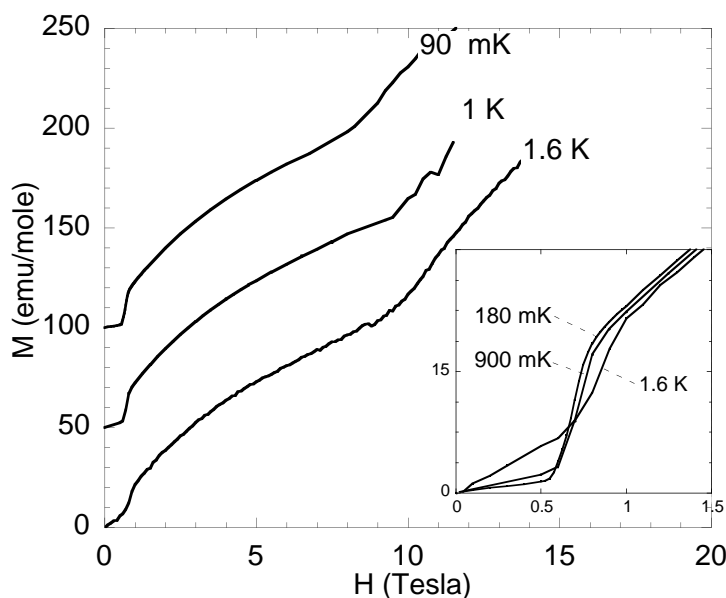


Figure 2. The magnetic field dependence of the magnetization M of $\text{Cu}_{0.98}\text{Zn}_{0.02}\text{GeO}_3$, at 1.6 K, 1 K, 200 mK and 90 mK. The curves are shifted along the y -axis. The inset shows the lower part of the diagram exhibiting the spin-flop transition (H is applied along the c -axis).

Above the spin-flop transition, the magnetization curves have a non-linear dependence on the magnetic field which may result from the formation of magnetic solitons at the impurity sites (as discussed in the last part).

2.2. The D-I transition line

Figure 3 shows the field dependence of M , measured at 1.6, 3, 5 and 7 K. The large increase of magnetization at around 9.5 T is associated with the phase transition between the D and I phases, similarly to the cases in previous reports for Zn-doped [13] and Si-doped [14] CuGeO_3 crystals.

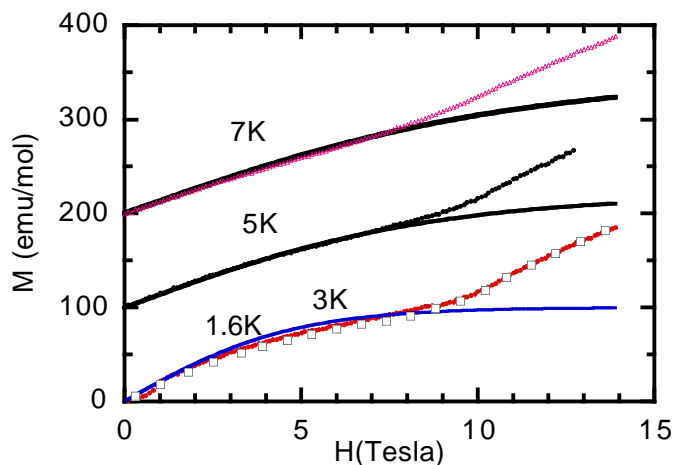


Figure 3. The magnetic field dependence of the magnetization M (H is parallel to the c -axis), at 1.6 K, 3 K, 5 K and 7 K. The solid curves are fits obtained using equation (1).

2.3. The AF–D and D–U transition lines

The AF transition is clearly detected at $T_N = 3$ K under 0.5 T as shown in figure 4, in agreement with the ultrasound results [17]. However, for higher fields applied along the c -axis, above the spin-flop transition, it can be seen that in figure 3 the magnetization does not show any sharp decrease, but shows a continuous broad increase as T is reduced to very low temperatures. Such a drastic change of the AF state with the magnetic field was also reported on the basis of specific heat measurements on a Si-doped crystal [11] and reveals the very specific character of the AF state coexisting with the SP dimerized state. At higher T , the drop in M/H corresponds to the occurrence of the dimerized state. The inset shows in more detail the variation of M near T_{SP} at different fields.

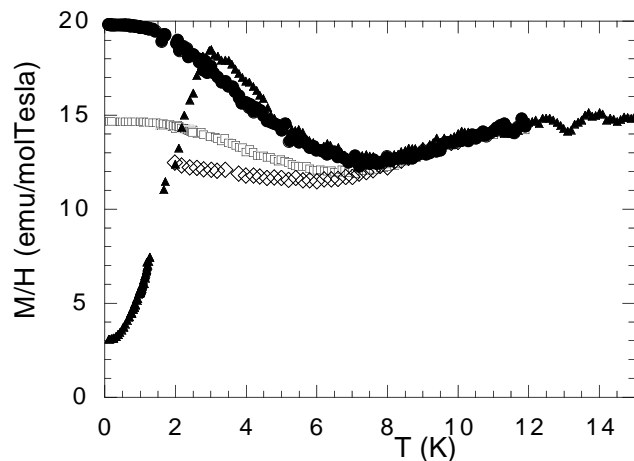


Figure 4. The temperature dependence of M/H at different constant applied magnetic fields (parallel to the c -axis) lower than H_c . \blacktriangle : 0.5 T; \bullet : 2 T; \square : 5 T; \diamond : 7 T.

2.4. The I'-I and I-U transition lines

In figure 5 the temperature variation of the magnetization is drawn for fields H higher than H_c , $H = 10, 11$ and 14 T. The drop in M/H at higher T_c corresponds to the I-U transition line. The transition temperature is determined by the maximum in the derivative dM/dH as shown in the inset of figure 5 for $H = 10$ T.

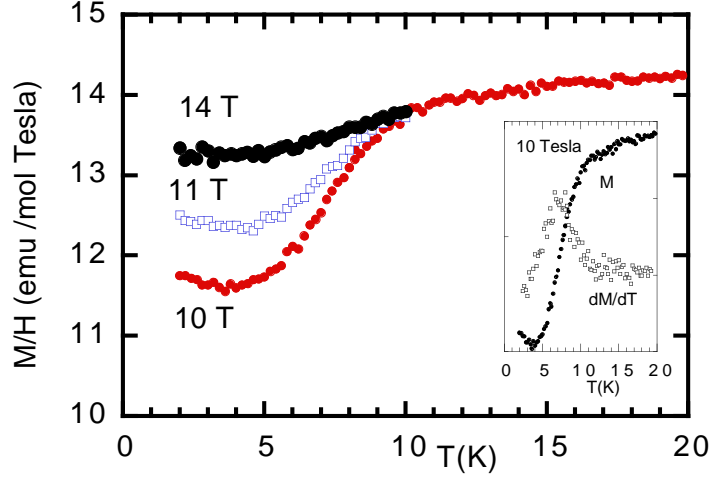


Figure 5. The temperature dependence of M/H at different constant magnetic fields larger than H_c . The inset shows $M(T)$ and the derivative dM/dT at 10 T.

No significant variation in $M(T)$ at fixed field can be associated with the I'-I transition. Such a transition, which was clearly observed in ultrasound measurements, should involve a very small (if there is any) magnetization jump.

All of the transition points obtained from our magnetization measurements are indicated on the phase diagram in figure 1.

3. Discussion and conclusions

The dimerization at zero field in a 2% Zn-doped CuGeO₃ crystal occurs at ~ 10 K, as compared with 14 K for the pure compound. Application of H reduces the energy gap by the Zeeman energy, until zero is reached at the critical field H_c . A universal curve for $gH_c/(2T_{SP}(0))$ versus $T/T_{SP}(0)$ has been shown to be followed by all SP compounds, g being the gyromagnetic factor in the field direction. With $T_{SP}(0)$ reduced from 14 to 10 K, H_c is also reduced from 14.5 T to 10 T in good agreement with our data.

For pure CuGeO₃, the dimerized (D) phase is non-magnetic, but above H_c the proliferation of magnetic solitons in the incommensurate I phase yields an increase of the magnetization. In the 2% Zn-doped CuGeO₃, a non-zero magnetization M_D is observed in the D phase (see figure 3). Such a behaviour is related to the free-1/2-spin field in the vicinity of each Zn impurity. Thus the magnetic field dependence of M_D above 3 K in the dimerized region (figure 3) can be relatively well described by a Brillouin function (\mathcal{B}_{ri}):

$$M_D = N\mu_B \mathcal{B}_{ri} \frac{\mu_B H}{k_B T} \quad (1)$$

where N is the number of magnetic moments μ_B . The relations content $y = N/N_{mol}$

used in (1) to fit the data from figure 3 are reported in table 1. It can be calculated that one 1/2 spin is associated with each Zn impurity, in agreement with the results given in references [12, 13].

Table 1. The parameter describing the magnetization in the dimerized phase, $y = N/N_{\text{mol}}$, for $N_{\text{mol}}\mu_{\text{B}} = 5585 \text{ emu mol}^{-1}$.

| | |
|-----|-------------|
| 3 K | $y = 0.025$ |
| 5 K | $y = 0.021$ |
| 7 K | $y = 0.026$ |

We have shown from our magnetization measurements that the incommensurate transition extends at low temperature into the AF state. Thus we have measured H_c down to 90 mK. The effect of magnetic field on the AF + SP coexistence states has been recently studied theoretically [20]: it was shown that, for dilute systems, the formation of solitons at the impurity sites will contribute to the magnetization $x\mu_{\text{B}}$ per site above a critical field $H_c(x)$ depending on the concentration x of impurities. Another jump of magnetization will occur at $H_c > H_c(x)$ due to solitons similar to those in pure compounds [20]. Our magnetization curves in the AF region are in good agreement with such a description, in particular as regards the non-linear field dependence of the magnetization above the spin-flop transition (figure 2). A weak-dilution analysis is appropriate for 2% Zn-doped CuGeO_3 , which has a separation of about 50 Cu–Cu distances between two Zn ions. This average impurity distance is much larger than the soliton length χ_0 for the pure system, evaluated to be ~ 12 Cu–Cu distances [7].

The soliton structure built when the field H is increased in magnitude beyond H_c from the dimerized phase or from the AF + SP phase is not essentially magnetically different; consequently the I–I' transition line detected by ultrasound measurements is not detected from our magnetization measurements. However, from figure 1 it is seen that, when H is increased, the I phase is more and more restricted in the phase diagram, to the benefit of the I' or AF phase, and disappears above $H = 15$ T above which the phase diagram between the I'–AF and U phases reduces to a vertical line at $T = 4.5$ K. It was shown that a sufficient doping totally suppresses the spin–Peierls phase and in this case the (H, T) phase diagram is a vertical line at $T \sim 4.5$ K separating an AF Néel state and the paramagnetic phases (see figure 4 in reference [11] for 2% Si-doped CuGeO_3). Thus it can be concluded that for doped CuGeO_3 samples, high magnetic fields destabilize the spin–Peierls state in its incommensurate phase and favour a pure AF state above a field of ~ 15 T.

Acknowledgments

One of us (PM) is indebted to H Fukuyama and M Saito for illuminating discussions.

References

- [1] Boucher J P and Regnault L P 1996 *J. Physique I* **6** 1939
- [2] Hase M, Terasaki I, Sasago Y, Uchinokura K and Obara H 1993 *Phys. Rev. Lett.* **71** 4059
Hase M, Terasaki I, Sasago Y, Uchinokura K and Obara H 1993 *Phys. Rev. B* **48** 9616
- [3] Lussier J G, Coad S M, McMorro D F and Paul D M^cK 1995 *J. Phys.: Condens. Matter* **7** L325
- [4] Hase M, Uchinokura K, Birgeneau R, Hirota K and Shirane G 1996 *J. Phys. Soc. Japan* **65** 1392
- [5] Sasago Y, Koide N, Uchinokura K, Martin M C, Hase M, Hirota K and Shirane G 1996 *Phys. Rev. B* **54** 6835

- [6] Regnault L P, Renard J P, Dhahenne G and Revcolevschi A 1995 *Europhys. Lett.* **32** 579
- [7] Kiryukhin V, Keimer B, Hill J P, Coad S M and Paul D M^cK 1996 *Phys. Rev. B* **54** 7269
- [8] Fukuyama H, Tanimoto T and Saito M 1996 *J. Phys. Soc. Japan* **65** 1182
- [9] Fabrizio M and Melin R 1997 *Phys. Rev. Lett.* **78** 3382
Fabrizio M and Melin R 1997 *Phys. Rev. B* **56** 5996
- [10] Manabe K, Ishimoto H, Koide N, Sasago Y and Uchinokura K 1998 *Preprint*
- [11] Hiroi M, Hamamoto T, Sera M, Nojiri H, Kobayashi N, Motokawa M, Fujita O, Ogiwara A and Akimitsu J 1997 *Phys. Rev. B* **55** R6125
- [12] Renard J P, LeDang K, Veillet P, Dhahenne A and Regnault L P 1995 *Europhys. Lett.* **30** 475
Grenier B, Renard J P, Veillet P, Paulsen C, Calemczuk R, Dhahenne G and Revcolevschi A 1998 *Phys. Rev. B* **57**
Grenier B, Renard J P, Veillet P, Paulsen C, Dhahenne G and Revcolevschi A 1998 *Preprint*
- [13] Hase M, Sasago Y, Terasaki I, Uchinokura K, Kido G and Hamamoto T 1996 *J. Phys. Soc. Japan* **65** 273
- [14] Nojiri N, Hamamoto T, Wang Z J, Mitsudo S, Motokawa M, Kimura S, Ohta H, Ogiwara A, Fujita O and Akimitsu J 1997 *J. Phys.: Condens. Matter* **9** 1331
- [15] Poirier M, Beaudry R, Castonguay M, Plumer M L, Quirion G, Ravazi F S, Revcolevschi A and Dhahenne G 1996 *Phys. Rev. B* **52** R6971
- [16] Fronzes P, Poirier M, Revcolevschi A and Dhahenne G 1997 *Phys. Rev. B* **55** 8324
- [17] Saint-Paul M, Hegman N, Reményi G, Monceau P, Dhahenne G and Revcolevschi A 1997 *J. Phys.: Condens. Matter* **9** L231
- [18] Kiryukhin V, Keimer B, Hill J P and Vigliante A 1996 *Phys. Rev. Lett.* **76** 4608
- [19] Revcolevschi A and Collongues R 1969 *C.R. Acad. Sci., Paris* **266** 1767
- [20] Saito M 1998 *J. Phys. Soc. Japan* **67** 2477